A. FINAL REPORT: DOE Award Number: DE-SC0004937, University of CA, San Diego

B. Bio-Inspired Routes for Synthesizing Efficient Nanoscale Platinum Electrocatalysts
PI: Jennifer N. Cha; Co-PI: Joseph Wang

C. 09/01/12-08/31/14

D. Executive Summary

Over the past three years, multiple accomplishments and major scientific advances have been achieved and these include the following: 1) synthesis of well defined platinum nanoparticles from a single platinum binding peptide; 2) synthesis of defined platinum nanoparticles from polymers that remain catalytically active for oxygen reduction reaction (ORR) without the need for any pretreatment or removal of organics; 3) controllable dispersion of platinum nanoparticles (PtNPs) throughout multilayers of a unique and highly ordered lithographically-patterned 3D porous carbon (PC) and grapheme substrates; 4) synthesis of defined platinum nanoparticles from the amino acid PEG polymers; 5) synthesis of amino acid functionalized polyethylene glycol (PEG) polymers to investigate the role of each amino acid for platinum binding, nanoparticle synthesis and catalysis; 6) development of powerful self-propelled nanomotors based on electrocatalytic platinum surfaces; 7) development of novel microporous electrode materials and nanoparticle supports for enhanced fuel performance; 8) development of bio-inspired catalytic nanomotors; 9) demonstrating that coupling specific amino acid "R" groups to polyethylene glycol (PEG) chains through amide bonds and adsorbing them to platinum (Pt) black led to improvements in oxygen reduction reaction (ORR) catalysis over bare metal, even at high polymer loadings. We describe these developments in detail below, as well as attach our list of products (15 publications describing these and additional advances).

Actual Accomplishments

(YEAR 1)

(1) In the first year of funded research, we published work on use of platinum binding peptides to synthesis platinum nanocrystals with tunable size and shape control. For the first time, we illustrated methods to generate platinum nanocrystals of controlled sizes and morphologies from a single peptide sequence simply by changing the rate of metal reduction. Peptides were isolated by screening phage libraries against single crystal Pt (100) surfaces to isolate peptides with preferential binding to the (100) face. Using the same peptide with different combinations of platinum precursors and reductants, we produced crystal morphologies ranging from 2 nm seed nuclei to 4 nm polyhedra to 7-8 nm cubes, all in aqueous media at room temperature and neutral pH. Figure 1.1 displays such cube morphologies that were achieved using this synthesis. The generation of truncated cube and cube morphologies is particularly exciting because the peptides were intended to bias the generation of peptides that bind to (100) planes. These discoveries therefore pose the possibility of controlling crystal morphology through peptide ligands that interact with specific crystal planes. The ability to use biomolecular recognition to tune crystal shape could be an exciting advance in nanocrystal synthesis. By synthesizing platinum nanocrystals with a variety of sizes and morphologies from a single peptide sequence, we illustrated in this work the first steps toward controlling platinum nanocrystal size and morphology using a biomolecular template. This work was published in *Chemistry of Materials* [1].

(2) In the first year, we also illustrated for the first time methods to generate platinum nanocrystals of controlled sizes and morphologies that also remain highly active for catalysis without the need for any pretreatment or removal of organics. While small molecules and polymers such as polyacrylic acid have been used successfully to generate controlled morphologies of nanoscale platinum, their binding strengths with the platinum surfaces often make it difficult for molecular adsorption, preventing catalysis. It is therefore of great importance to discover moieties that can both synthesize controlled platinum structures that are still able to desorb from the nanoparticles in working conditions. In this report, we demonstrate that simple short linear chains of polyethyleneglycol (PEG) can be used to synthesize well-defined sub-10 nm platinum cubes and truncated cubes. We furthermore show that platinum nanoparticle growth is controlled through the terminal hydroxyl groups on the PEG (OH-PEG-OH) chains that oxidize during or post platinum nanoparticle synthesis. Because only the groups at the termini of the polymers are at the platinum surface, in working electrolytes such as H_2SO_4 these weak carbonyl-platinum interactions dissociate easily, allowing for effective catalysis of reactions such as oxygen reduction reaction (ORR). Finally, surface studies demonstrated that while facile dissociation of the polymers from the platinum substrates is possible because only the end groups bind platinum, the end groups used and the molecular weight of the polymers can make a marked difference in both synthesis and ORR activity. This work has been published in *Journal of Materials Chemistry* [2].

Concurrent to these research efforts, ORR studies using platinum nanocrystals synthesized from the platinum binding peptides, as opposed to polymers outlined above, showed very poor activity, indicating that the peptides cannot dissociate away from the platinum surfaces during electrochemical cycling. This is most likely due to specific amino acids oxidation or reduction during particle synthesis leading to strong peptide-platinum interactions, thereby making it difficult for oxygen binding and reduction. Detailed studies using individual amino acids and the PEG polymers as stabilizing macromolecules for both platinum synthesis as well as catalysis are currently underway. *These studies are critical if bio-enabled platinum synthesis is to be used for platinum catalysis, including ORR.*

(3) We demonstrated the controllable dispersion of platinum nanoparticles (PtNPs) throughout multilayers of a unique and highly ordered lithographically-patterned 3D porous carbon (PC) substrate [3]. The resulting hierarchical structure allowed for high mass transport access and catalytic activity for a diverse range of applications. Control of the electrodeposition conditions offered tailoring of the size and morphology of the PtNPs, along with narrow size distributions, and hence control of the electrochemical behavior. The decoration of PtNPs over the highly ordered 3-D carbon structure are shown in Figure 1.1. Such incorporation of PtNPs onto a 3D carbon nanostructure led to high chemical and mechanical stability with improved mass transport profiles. The coupling of the catalytic properties of PtNPs with the attractive structural regularity and rigidity of 3D PC offers considerable promise for diverse applications such as fuel cells, flow sensors, remediation, and biosensors.

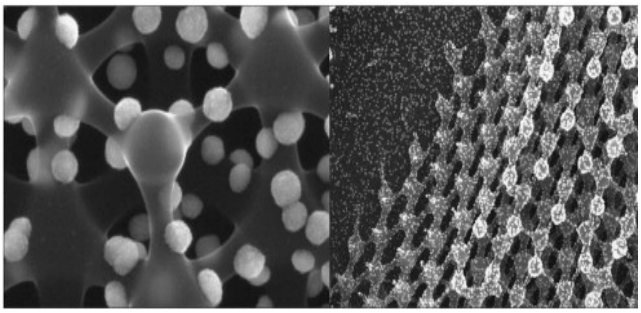

Figure 1.1: *Dispersed Pt nanoparticles over ordered 3-dimensional carbon structure* (ref 3).

(4) Some of our activity has involved the development of powerful self-propelled catalytic nanomotors based on platinum surfaces. These new microtube rockets are based on electro-chemical growth of conical bilayer polyaniline (PANI)/platinum microtubes within the

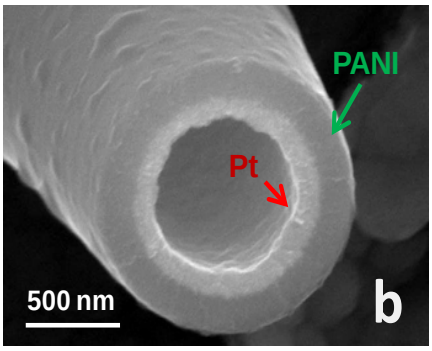

Figure 1.2. *Template-prepared polyanoline/Pt bilayer microtube engines [Ref 4].*

conically-shaped pores of a polycarbonate template membrane [4]. Propulsion is achieved by electrocatalytic reaction of the peroxide fuel at the inner Pt surface. These mass produced microtubular engines are only 8 μm long, move at an ultrafast speed (of over 300 body-lengths s^{-1}), and can operate in very low (down to 0.2%) levels of the hydrogen peroxide fuel. A schematic of the self-propelled nanomotors is shown in Figure 1.2. The propulsion characteristics and optimization of these microtubular engines have been described, along with their efficient operation in different biological environments that holds great promise for biomedical applications.

Finally, we developed a hybrid nanomotor, combining chemically-powered propulsion and a magnetically-driven locomotion [5]. The new catalytic-magnetic nanomotor consists of a flexible multi-segment Pt-Au-Ag_{flex}-Ni nanowire, with the Pt-Au and Au-Ag_{flex}-Ni portions responsible for the catalytic and magnetic propulsion modes, respectively. The experimental data and theoretical considerations indicate that the new hybrid design only minimally compromises the individual propulsion modes. Rapid and convenient switching from the catalytic to the magnetic mode is illustrated in Figure 1.5. The resulting catalytic-magnetic adaptive nanomotor can address the fuel depletion and salt limitation common to chemically-powered motors by switching to a magnetic propulsion.

(YEAR 2)

Major accomplishments during the second year include 1) synthesis of amino acid functionalized polyethylene glycol (PEG) polymers to investigate the role of each amino acid for platinum binding, nanoparticle synthesis, and catalysis; 2) synthesis of defined platinum nanoparticles from the amino acid PEG polymers; 3) development of novel microporous electrode materials and nanoparticle supports for enhanced fuel performance; and 4) development of bio-inspired catalytic nanomotors.

(1) Synthesis of amino acid functionalized polyethylene glycol (PEG) polymers: In the second year of funding, we completed studies analyzing the use of simple short linear chains of polyethylene glycol (PEG) to synthesize well-defined sub-10 platinum nanoparticles, including cubes and truncated cubes. We furthermore determined that the **platinum nanoparticle growth was controlled through the terminal hydroxyl groups on the PEG** (HO-PEG-OH) chains that oxidized to carbonyl groups during or after synthesis. *When dimethoxy PEG was used in place of HO-PEG-OH, uncontrolled platinum synthesis occurred to generate bulk platinum precipitates.* Because only the OH groups at the termini of the polymers influenced particle synthesis and growth, in working electrolytes such as H_2SO_4 the weak carbonyl-platinum interactions could dissociate easily, allowing for effective catalysis of reactions such as oxygen reduction reaction (ORR) without any pretreatment. Finally, surface studies also demonstrated that the end groups of the PEG chains as well as the polymer molecular weight could make a significant difference in both synthesis and ORR activity. For example, while amine terminated PEG produced defined Pt nanostructures, IR studies confirmed that the amine-Pt interactions were too strong to dissociate easily in acid, decreasing the net ORR activity for the amine-PEG particles. Furthermore, larger molecular weight PEG-OH exhibited

poor control over nanoparticle synthesis and low dissociation kinetics from the particle surfaces. This work was published in *Journal of Materials Chemistry* in 2011 [1].

(2) Synthesis of defined platinum nanoparticles from the amino acid PEG polymers. Because spectroscopic and synthesis experiments showed that the ethylene oxide backbone of PEG did little to influence platinum nanoparticle nucleation and growth, these polymers became ideal substrates and scaffolds upon which to attach amino acid R groups in order to investigate specific amino acid-platinum interactions with respect to both synthesis and catalysis. Typically, biomediated syntheses of inorganic nanocrystals require multi amino acid peptides, making it very difficult to discern the effect of each individual amino acid or R group on metal or crystal binding. Because of this, while others have considered using amino acids as ligands to influence particle nucleation and growth, little progress has been made in actually implementing specific amino acid-inorganic interfaces for this purpose. However, to obtain active catalysts from peptide or protein-based templates it is imperative to perform fundamental studies to investigate the chemical nature of the amino acid-inorganic interface and the strength of these interactions.

In order to investigate individual amino acid-Pt interactions, PEG chains were end-functionalized with specific amino acid R groups. Because many polar moieties can also bind platinum and affect both synthesis and catalysis, simple amines composed of a primary amine on one end and the R group on the other (i.e. decarboxylated amino acids) were used to isolate the effect of R group binding,. Specifically, N-hydroxysuccinimide functionalized low molecular weight PEG was reacted with (W) Tryptamine, (R) Agmatine sulfate, (H) Histamine, (F) Phenethylamine, (Y) Tyramine, (V) Isobutylamine, (E) 4- aminobutyric acid, (S) Ethanolamine, (T) Amino-2-propanol, (C) Cystamine dihydrochloride and (Q) 4-Aminobutyramide Hydrochloride in DMF and/or water. After reaction, the solvent was evaporated and the dried film/solid was then resuspended in water and dialyzed to remove excess amine and N-hydroxysuccinimide. Because some of the amines with aromatic R groups, such as tryptophan and phenylalanine, were not soluble in water, the corresponding R group functionalized PEG chains were also not completely soluble in water and were thought to phase separate into micellar or vesicle structures. After dialysis, the R group functionalized PEG polymers were separated from hydrolyzed PEG-NHS (or PEG-COOH) and any remaining amines by using preparatory thin layer chromatography (Prep TLC). To date, PEG-W, PEG-H, PEG-R, PEG-F and PEG-Y have been successfully synthesized and purified using these procedures (Figure 2.1), while synthesis and purification of PEG-S, PEG-T, PEG-V, PEG-E and PEG-Q are in progress. While most of these syntheses are expected to proceed smoothly, due to the similarity in end groups between PEG-E and hydrolyzed PEG-NHS (e.g. PEG-COOH), it may be challenging to completely isolate only PEG-E. Most of these amino acids were chosen based on the initial consensus sequences obtained from phage display screening against platinum cubes (Year 1) –" Y H **P W** N A **Q R E L S V**", literature precedence that used either threonine rich sequences or phenylalanine peptides also drove studying platinum interactions with PEG-T and PEG-F. Again, unlike these other studies though, for the first

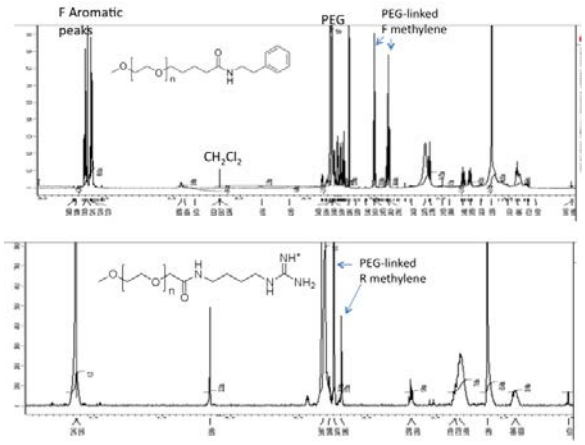

Figure 2.1. *NMR spectra confirming successful synthesis and purification of PEG-phenylalanine and PEG-arginine.*

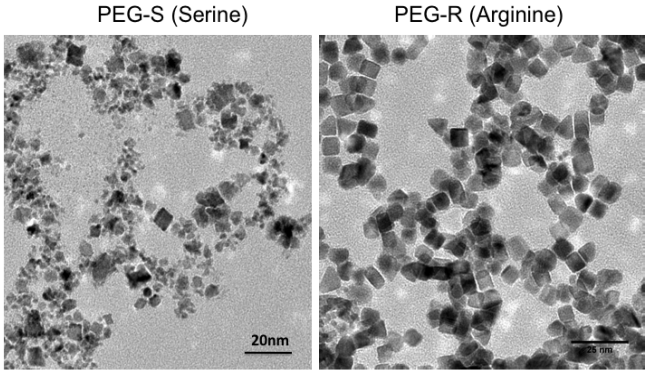

Figure 2.2. *Platinum nanoparticles synthesized from PEG-Serine (left) and PEG-Arginine (right)*

time it is hoped that we can gain a fundamental understanding of the individual amino acid alone, as opposed to potential complications caused by close proximity to other amino acids.

The successfully synthesized R group functionalized PEG polymers were next reacted with overnight aged platinum (K_2PtCl_4) solutions and reduced with hydrogen. Because PEG-W and PEG-F were not soluble in pure water, a mixture of DMF and water was used. As a control, 60:40 DMF:water (v/v) containing either no PEG or the initially studied PEG200 (which gave Pt cubes previously) only were tested in platinum reactions. In the absence any ligands, using a 60:40 DMF:water mixture gave aggregates of small (3-4 nm) spherical Pt particles indicating that DMF alone can play a role on particle nucleation and growth. Furthermore, with PEG200 in 70:30 water:DMF, very different Pt nanoparticle morphologies formed than if the reactions were run in pure water. Clearly, the effect of solvent on particle synthesis becomes important in mixed organic/aqueous solvent systems, and this is currently being investigated further. Starting from TLC-purified PEG-F, PEG-W, PEG-R or PEG-H, platinum reactions were run in either pure water or DMF/water mixtures. In all cases, 0.001 M K_2PtCl_4 solutions aged overnight were mixed with 100mM concentrations of the PEG polymers and reduced in H_2 overnight. As shown in Figure 2.2, the polar PEG-R and PEG-S polymers generated cubic nanoparticles, whereas the aromatic PEG-W and PEG-H produced more ill-defined and aggregated dendritic structures. Since polymer solubility, potential microscopic phase separation, and solvent alone can also affect platinum nanocrystal synthesis, more careful synthesis and spectroscopic analyses must be done prior to elucidating the exact role of each amino acid R group on platinum particle synthesis and catalysis. PEG-V, PEG-S, PEG-T, and PEG-E have also been synthesized and purified. These will also be combined with aged Pt solutions and reacted to form Pt nanostructures, two of which are shown in Figure 2.3. These developments were published in the *J. Mater. Chem*. [6].

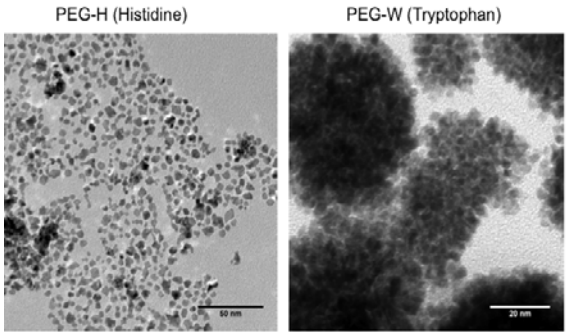

Figure 2.3. *Pt nanoparticles synthesized from PEG-Histidine (left) and PEG-Tryptophan*

(3) Development of novel micrporous electrode materials for enhancing the performance of fuel cells. Several accomplishments involving new and advanced electrode materials and nanoparticle supports for fuel cell applications have been achieved during the second year, including:

A) The preparation and characterization of highly ordered tailored 3D hierarchical nano/microporous gold–carbon architectures. We have designed and prepared three-dimensional hierarchical architectures, consisting of monolithic nanoporous gold or silver films formed on highly ordered 3D microporous carbon supports. Unique biomimetic nanocoral- or

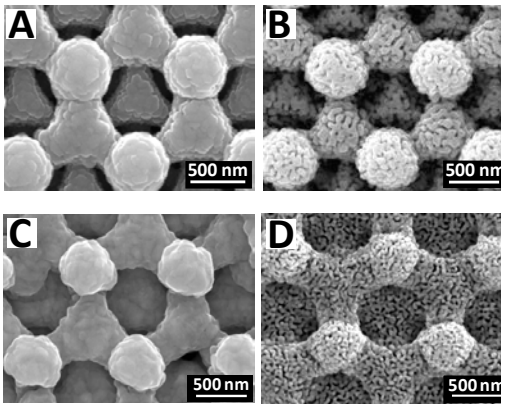

Figure 2.4. *SEM images of Ag/Al alloy film (A), porous Ag (B), Ag/Au alloy film (C) and porous Au on the 3D porous carbon (D)*

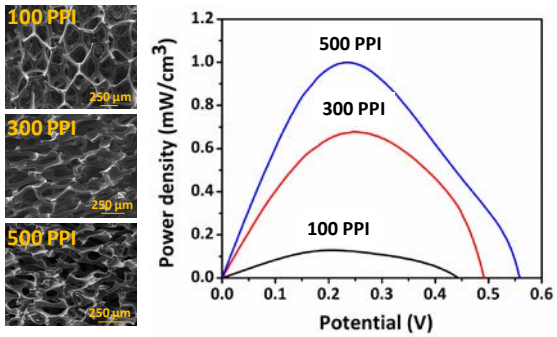

Figure 2.5. *SEM images of the RVC substrates for 100 ppi, 300 ppi and 500 ppi (Left). Power density from the different RVC supports (Right).*

nanocauliflower-like self-supporting structures have been formed, depending on the specific preparation conditions, as was demonstrated using SEM. We demonstrated that such architectures significantly enhance the performance of fuel cells and biofuel cells. The formation of the new nano/microporous structures involves the electrodeposition or sputtering of metal alloys onto the lithographically patterned multi-layered microporous carbon, followed by preferential chemical dealloying of the less noble component. The resulting hierarchical structure displays a highly developed 3D interconnected network of micropores with a nanoporous metal coating as shown in Figure 2.4. The nanoporosity of the metal films and the diameter of the large micropores have been tailored by systematically changing the alloy compositions via control of the deposition potential, plating solution and coarsening time. The new 3D hierarchical nano/microporous architectures allow for enhanced mass transport and catalytic activity compared to common nanoporous films prepared on planar substrates. The functionality of this new carbon–gold hierarchical structure was illustrated from the substantially higher power output of the corresponding fuel cells, compared to the bare microporous carbon substrate. This work was published in *Journal of Materials Chemistry* [7].

B) Fuel Cells based on high-surface area reticulated vitreous carbon (RVC). In this effort we investigated the utility of new 3D highly dense open-cellular microstructure reticulated vitreous carbon (RVC) as a porous substrate support for fuel cell applications. Three different geometrical pore sizes, 100, 300 and 500 pore per inch (ppi), of the carbon foam were successfully tested as a porous substrate. The anode material comprised of methylene blue (MDB) as a mediator and an enzyme, glucose dehydrogenase (GDH) for glucose oxidation, while Pt black with CNTs-PLL-laccase was used for cathode construction. Figure 2.5 shows SEM images of the RVC substrates from 100 to 500 ppi (left) along with the corresponding power density curves. The new highly densed 500 ppi RVC material exhibits a maximum power density of 1 mW/cm^3 and an open circuit voltage of 560 mV under the flow rate of 2 µL/min. This work has been submitted for publication.

C) This effort introduces highly-ordered 3D microporous carbon and graphene nanoparticle supports for oxygen reduction and direct methanol fuel cell (DMFC) technology. Alloy nanoparticles (Pt/Ru or Pt/Pd) on the new porous carbon supports displayed efficient electrocatalytic activity for fuel cells applications. Such Pt/Ru or Pt/Pd alloy nanoparticles were electrodeposited onto the 3D microporous carbon supports, as illustrated in the SEM images of Figure 2.6. Figure 2.6A shows Pt/Ru nanoparticles distributed evenly throughout the 3D

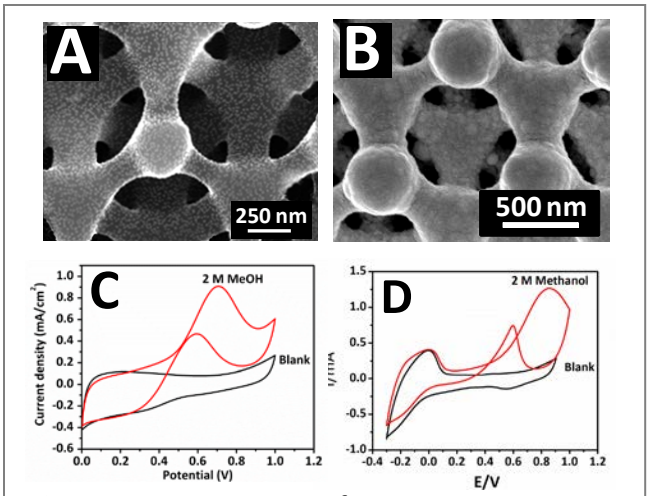

Figure 2.6. *SEM images of a 3D microporous carbon electrode decorated with Pt/Ru (A) or Pt/Pd (B) nanoparticles; CVs for the oxidation of 2 mM methanol by Pt/Ru nanoparticles(C) or Pt/Pd (D). on the 3D microporous carbon electrodes in 0.5 M H_2SO_4.*

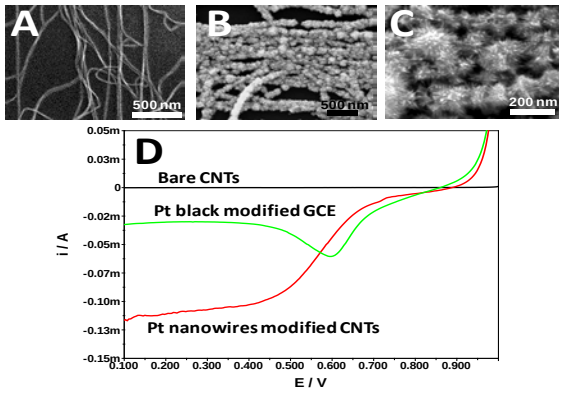

Figure 2.7. *SEM images of multiwall carbon nanotubes stretched on the substrate (A), urchin-like Pt nanowires on multiwall carbon nanotubes (B), magnified image of B (C). Also shown (D) are ORR voltammograms at the urchin-like Pt nanowires (Red) and Pt Black modified electrode (green).*

microporous carbon support (average particles size of 15 nm). Figure 2.6B displays Pt/Pd film on 3D microporous carbon. The fully exposed surface of this new 3D carbon material has the potential for enhanced access of electrolyte solution to the nanoparticles without agglomeration. Figures 2.6C and D display cyclic voltammograms of methanol oxidation in acidic media using Pt/Ru nanoparticles or Pt/Pd film on modified 3D microporous carbon supports, respectively.

C) In another research direction, we have demonstrated the electroless plating of sea urchin-like Pt nanowires on MWCNTs. The electrocatalytic activity of the new nanostructures toward the oxygen reduction reaction (ORR) was examined. Figure 2.7 displays SEM images of MWCNTs stretching along the substrate (A) and of MWCNTs after plating the Pt nanowires (B and C). Urchin-like Pt nanowires can be observed all over MWCNTs (B and C). The electrocatalytic activity of the resulting urchin-like Pt nanowires on MWCNTs for ORR was illustrated (D). These ORR results (D) indicate a high electrocatalytic activity of urchin-like Pt nanowires, comparable to that of standard Pt black.

D) Water-splitting catalytic reactions and materials, offering extended motor lifetimes and/or higher efficiency, are highly desired for future water-driven nanomotor operations. We have presented the first example of chemically powered micromotors propelled autonomously using water as the sole fuel source [8]. While the water-splitting reaction was used before to drive bipolar-electrochemical macroscale motors under an external electrical field, it has not been used for the locomotion of self-propelled chemically powered micromotors. The water-splitting reaction, involving Al–Ga alloys, has been used for realizing such water-driven microscale motion, with the reaction and propulsion efficiencies improving *via* the liquid metal embrittlement in the Al–Ga system. The presence of such a liquid phase in the alloy microstructure facilitates the continuous hydrogen-generating reaction between aluminum and water. We have demonstrated that the resulting water-driven Al–Ga/Ti micromotors can swim in water at 150 body lengths per second, as well as in biological media such as human serum. Further improvements in the propulsion behavior are expected by enhancing the alloy reactivity *via* a judicious control of its microstructure and composition.

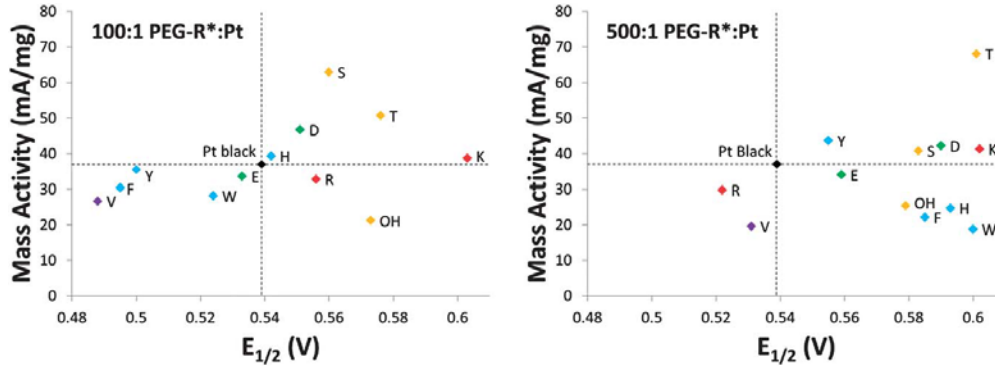

Figure 3.1. *Plots of mass activity (mAmg1) versus half wave potential (E1/2) for PEG–X coated Pt black at (left) 100 : 1 molar ratios of PEG–X : Pt and at (right) 500 : 1 molar ratios of PEG–X : Pt.*

YEAR 3

(1) In the final year of funding, we demonstrated that coupling specific amino acid "R" groups to polyethylene glycol (PEG) chains through amide bonds and adsorbing them to platinum (Pt) black led to improvements in oxygen reduction reaction (ORR) catalysis over bare metal, even at high polymer loadings. Through our studies, we first show that the presence of PEG on the Pt nanoparticles increases half-wave ($E_{1/2}$) potentials, most likely by preventing Pt oxidation or Pt-OH formation. We also show however that increases in $E_{1/2}$ did not necessarily correlate to gains in mass activities, and that while commercial PEG-OH in fact lowered mass activities, conjugation of PEG to alcohol-containing amino acid R groups connected by amide bonds led to 100-200% gains in reactivity. The relationship between E1/2 and mass activities relative the R-group are shown in Figure 3.3. This work presents evidence that counters the common conception that organic capping ligands decrease catalytic activity; in fact activity may actually be improved over bare metal through judicious choice and design of ligands that inhibit Pt oxidation and control chain packing at the Pt surface. These studies therefore show that it may still be possible to have ligands on a nanoparticle surface that allow the particles to be well-dispersed on an electrode surface while simultaneously enhancing catalysis without further particle treatment.

(2) We have also demonstrated a multilayered highly ordered three-dimensional (3D) graphene structure that served as an attractive support for catalytic metal nanoparticles [9]. Different metal nanostructures modified 3D graphene, *i.e.*, Pd, Pt and Au, have been successfully illustrated (Figure 3.2). The morphology, distribution and sizes of these nanoparticles on the 3D graphene support have been tailored by changing the preparation conditions. Pt nanostructures with nanospike and nanoparticle shapes have thus been prepared, along with cube-shaped Pd nanoparticles and nanoflower- and spherical shaped Au nanostructures. Enhanced electrocatalytic activity towards ORR and hydrogen peroxide has been demonstrated. The catalytic activity toward ORR of Pt NPs on 3D graphene compared

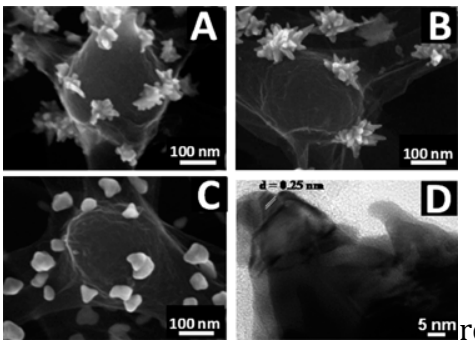

re

Figure 3.2. Effect of Au concentration upon the shape of Au NPs on 3D graphene. $HAuCl_4$ concentration: (A) 0.1 mM, (B) 0.5 mM and (C) 1 mM. All Au NPs were deposited by cycling the potential for 1000 cycles. (D) TEM image of (B). [91.

favorably to that of Pt NPs on a 3D carbon substrate and on a glassy carbon electrode, bare 3D graphene and Pt black. The voltammetric results clearly demonstrate the excellent electrocatalytic activity of Pt NPs on 3D graphene catalysts for oxygen reduction. Similarly, Pd NPs on 3D graphene display a greatly enhanced catalytic activity toward hydrogen peroxide compared to bare 3D graphene. Such metal nanoparticles decorated multi-layer 3D graphene allows for high mass transport access and catalytic activity for a diverse range of applications, including sensor and fuel-cell technologies.

(3) We demonstrated the combination of sphere lithography, template deposition with alloy-etching processes for preparing tailored-made 3D hierarchical macro/mesoporous gold architectures [10]. Fine control of the morphology and porosity of the new macro/mesoporous structures has been achieved by controlling the dimensions of the sphere template, the composition of the plating mixture solutions and the etching conditions. PS spheres were infiltrated into the polycarbonate membrane (PC) pores followed by the electroplating of Au/Ag over the PS spheres template. Dealloying of the Ag component and removal of the template resulted in macro/mesoporous gold wires featuring a honeycomb textured macroporous structure combined with a continuous sponge-like morphology. The new double templated electrodeposition method provides an attractive route for preparing highly controllable multiscale porous materials and diverse morphologies based on different materials and hence holds considerable promise for designing electrocatalytic or bioelectrocatalytic surfaces for a variety sensing and energy applications.

E. Products

1. L.M. Forbes, A.P. Goodwin, J.N. Cha Tunable size and shape control of platinum nanocrystals from a single peptide sequence, *Chemistry of Materials,* 2010, 22, 6524-6528.

2. Lauren M. Forbes, A. M. O′Mahony , S. Sattayasamitsathit, Joseph Wang and Jennifer N. Cha, "Polymer end-group mediated synthesis of well-defined catalytically active platinum nanoparticles", *J. Mater. Chem.* **21,** 15788-15792 (2011)

3. S. Sattayasamitsathit**,** A M. O' Mahony, X. Xiao, S. M. Brozik, C. M. Washburn, D. R. Wheeler, J. Cha, D. B. Burckel, R. Polsky and J. Wang, "Highly Dispersed Pt Nanoparticle-Modified 3D Porous Carbon: A Metallized Carbon Electrode Material", *Electrochemistry Communications*, 2011, 13, 856-860.

4. W. Gao, S. Sattayasamitsathit, J. Orozco and J. Wang, Highly Efficient Catalytic Microengines: Membrane Electrodeposition of Bilayer Polyaniline-Platinum Conical Microtubes, *J. Am. Chem. Soc., 2011,* 133, 11862–11864.

5. W. Gao, K. M. Manesh, J. Hua, S. Sattayasamitsathit and J. Wang*,* Hybrid Nanomotor: Catalytically/Magnetically Powered Adaptive Nanowire Swimmer, *Small,* 2011, 7, 2047-2051.

6. L.M. Forbes, S. Sattayasamitsathit, P.F. Xu, A. O'Mahony, I.A. Samek, K. Kaufmann, J. Wang, J.N. Cha, Improved Oxygen Reduction Reaction Activities with Amino Acid R Group Functionalized PEG at Platinum Surfaces, *J. Mater. Chem.* **1,** 10267 – 10273 (2013)

7. S. Sattayasamitsathit, A. M. O'Mahony, X. Xiao, S. M. Brozik, C. M. Washburn, D. R. Wheeler, W. Gao, S. Minteer, J. Cha, D. B. Burckel, R. Polsky and J. Wang, Highly ordered tailored three-dimensional hierarchical nano/microporous gold–carbon architectures. *J. Mater. Chem*., 2012, 22, 11950-1956.

8. W. Gao, A. Pei, J. Wang , Water-Powered Micromotors. *ACS Nano*, 2012, 6, 8432-8438.

9. S. Sattayasamitsathit, Y. Gu, K. Kaufmann, W. Jia, X. Xiao, S. Minteer, J. Cha, D. B. Burckel, C. Wang, R. Polsky, J. Wang, "Highly-Ordered Multilayered 3D Graphene Decorated with Metal Nanoparticles", *J. Mater. Chem. A,* 1, 1639-1645(2013).

10. S. Sattayasamitsathit, Y. Gu, K. Kaufmann, S Minteer, R Polsky, J Wang, Tunable hierarchical macro/mesoporous gold microwires fabricated by dual-templating and dealloying processes, *Nanoscale*, 2013, 5, 7849-7854.

11. Albert M. Hung, Nathan A. Konopliv, Jennifer N. Cha, "Solvent-Based Assembly of CdSe Nanorods in Solution", *Langmuir*, **27,** 12322-12328 (2011)

12. Albert M. Hung, Taeseok Oh, Jennifer N. Cha, "Facile Thermal Treatment Process for Assembling Vertically Aligned Semiconductor Nanorods in Solution", *Nanoscale*, 2012, 4, 1016-1020.

13. P.F. Xu, A.M. Hung H. Noh, J.N. Cha "Switchable Nanodumbbell Probes for Analyte Detection", *Small* 9, 228–232 (2013)

14*.* P.F. Xu, J.H. Lee, C. Choi, S. Jin, J. Wang, J.N. Cha, "Enhanced Raman Signals from Switchable Nanoparticle Probes", *Chem. Comm.,* 49, 8994-8996 (2013)

15. P.F. Xu, H. Noh, J.H. Lee, D.W. Domaille, M. Nakatsuka, A.P. Goodwin, J.N. Cha, "The Role and Potential of DNA for Next-Generation Materials", *Materials Today,* 16, 290-296 (2013).